Appl. Phys. B 65, 475–480 (1997)

Applied Physics B Lasers and Optics

Ionization via an ultrashort high-power KrF laser

A. Sagisaka, Y. Nabekawa, K. Kondo*, S. Watanabe

Institute for Solid State Physics, University of Tokyo, Roppongi 7-22-1, Minato-ku, Tokyo 106, Japan
(Fax: 03-3401-5169, E-mail: sagisaka@evans.issp.u-tokyo.ac.jp)

Received: 10 January 1997

Abstract. We present the systematic experimental results of photoelectron spectra of Ar, Ne, and He in a strong KrF laser field. Above-threshold ionization (ATI) peaks up to the 6th order were clearly observed and the positions of ATI peaks, including substructure, did not shift with laser intensity. These facts can be explained by the multiphoton resonance with Rydberg states. At a higher intensity, the continuum builds up but the ATI structure is still apparent. Eventually, even this structure is buried in the continuum, implying the tunneling regime.

PACS: 32.00

Ionization in a strong laser field has recently attracted interest in field-driven X-ray lasers [1–3]. This has been investigated extensively and, for various wavelengths, the intensity-dependence of ion yield and electron-energy spectra have been observed and compared with the calculation.

In general, ionization under a strong field is divided into two regimes, multiphoton and tunneling ionization. These two regimes are usually distinguished by the Keldysh parameter $\gamma = (I_P/2U_P)^{0.5}$, where I_P is the atom (or ion) ionization potential and U_P is the ponderomotive potential, given by $U_P = e^2E^2/4m\omega^2$ (e and m are the electron charge and mass, and E and ω are the field strength and frequency) [4]. The multiphoton regime corresponds to $\gamma \gg 1$, and the tunneling regime to $\gamma \ll 1$. The multiphoton character is evident in the photoelectron spectra as discrete peaks by the photon energy: above-threshold ionization (ATI). The γ parameter is actually a fairly good figure for discriminating two regimes in the red wavelength region. Mevel et al. [5] observed the evolution from multiphoton to tunneling ionization from the photoelectron spectra by changing the laser intensity, which interacts with atoms, effectively, over a wide range throughout all rare gases. In the longer wavelength (1 μm), ionization occurs by the suppression of the Coulomb potential rather than by tunneling [6].

In the UV wavelength region, ionization has been investigated in the multiphoton regime [7, 8]. Luk et al. [9] reported the photoelectron spectra using a short-pulse KrF laser. The widths of ATI peaks increased with the laser intensity. They explained the broadening of ATI peaks by the ponderomotive shift combined with the dynamics of ion population. In this case, they assumed that non-resonant ionization was dominant. Gibson et al. [10] on the other hand, reported the resonant ionization in Ar using a short-pulse XeCl laser. Some resonances with the Rydberg series were observed, and the position and width of the ATI peaks did not change in the intensity range investigated. This fact was explained by the three-photon resonance to the s states and the four-photon resonance to the f states due to the ac-Stark effect which occurred at a certain laser intensity, regardless of the peak intensity. The two experimental reports contradict each other in the ionization process.

In this paper, we present the systematic experimental results of photoelectron spectra in a strong KrF laser field with Ar, Ne, and He as target media. The ATI peaks were clearly observed and the position of ATI peaks did not shift with the laser intensity under investigation, although the positions are offset from those of $Nh\nu - I_P$ (N is the absorbed photon and $h\nu$ is the photon energy). These facts can also be explained by the Stark-induced resonances [10]. At a higher intensity, the continuum builds up, but the ATI structure is still apparent. Eventually, even this structure is buried in the continuum. This observation shows that the evolution from the multiphoton to the tunneling ionization occurs according to the γ parameter in the UV wavelength as well as in the longer wavelength.

1 Experiment

An ultrashort, high-power KrF laser was used at 10 Hz. The typical energy and the pulse width were 20 mJ and 300 fs, respectively. The laser system is similar to that used in [11]. The KrF amplifier was replaced by a relatively compact one with

*Permanent address: Center for Tsukuba Advanced Research Alliance (TARA), Institute for Material Science, University of Tsukuba, Tennodai 1-1-1, Tsukuba, Ibaraki 305, Japan

a 5 cm aperture for this experiment. The laser pulse was focused by the two achromatic lenses with focal length of 300 and 150 mm in a vacuum chamber. The typical full width at a half maximum (FWHM) of the spot was 7 μm, when we used the $f = 300$ mm lens. In the high-intensity region, an off-axis parabolic mirror ($f = 125$ mm) was used to avoid chromatic and spherical aberrations. The typical spot size (FWHM) was 3.5 μm. When a Gaussian spatial profile was assumed, the peak intensity was estimated as $0.61E/(\tau\pi r^2)$, where E is the laser energy, τ is the pulse width (FWHM), and r is the spot radius. This estimate, however, may contain some uncertainties, because the full energy was not always concentrated in the central part of the spatial and temporal profiles. Therefore, the intensity was calibrated by the resonance in Ar as described later.

The ion yields of He^+, Ne^+, and Ar^+ were measured with a time-of-flight (TOF) analyzer (R.M. Jordan Co.) in the setup described in [12, 13]. The rare gases were backfilled in the target chamber to a pressure of 4.7×10^{-7} torr after the chamber was evacuated below 5.0×10^{-9} torr. The electron energy spectra were measured with a TOF spectrometer in the setup described in [14, 15]. The detection cone angle was determined from the geometry and the effective area of the MCP, and was 3.6°. To decrease the background contamination, the vacuum chamber was evacuated below 8.0×10^{-9} torr with baking. Each rare gas was backfilled to a pressure between 1.0×10^{-7} and 3.7×10^{-6} torr. He, Ne, and Ar were used as target media, and the purity of these gases was better than 99.998 % in this experiment. The temporal profile of the electron yield, detected by a high-speed microchannel plate (MCP: Hamamatsu Model F3654-21s), was recorded by a digital signal analyzer (Tektronix DSA 602). The signals were accumulated only when the laser intensity was within ±5% of the desired value and were averaged over the shot number, above which the signal shape does not change anymore. The typical shot number was 32.

A typical TOF spectrum of Ne is shown in Fig. 1. The numbers show the order of the ATI peaks. A signal appeared even when no target gas was in the chamber. In particular, the signals of the H_2O-related electrons became stronger in the KrF laser light than those in the longer-wavelength laser light because the large photon energy (5 eV) of KrF laser light can easily dissociate H_2O. We first recorded the signal without the target gas and subtracted this value from the signal with the target gas. The temporal profile was transformed to the energy spectrum. With this procedure, we successfully obtained the photoelectron energy spectra.

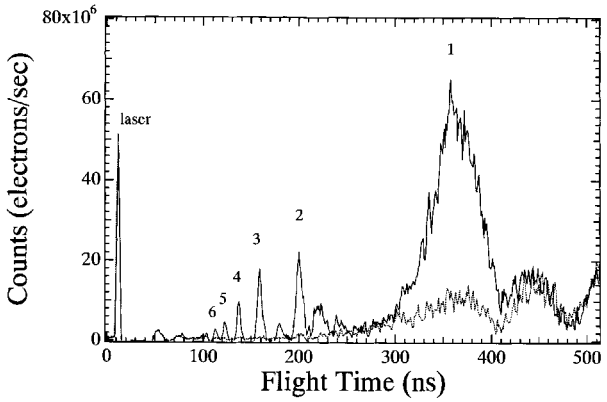

Fig. 1. TOF spectrum of Ne. The numbers show the orders of the ATI peaks. The first peak is the scattering light of the laser. The solid line shows the signal with the target gas. The dotted line shows the signal without the target gas

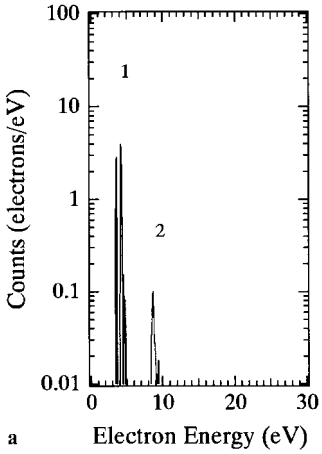

a

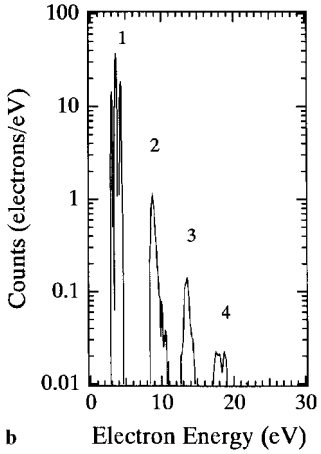

b

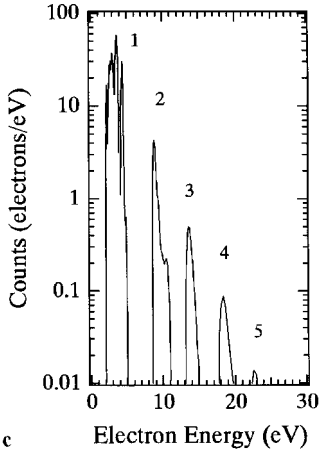

c

Fig. 2a–c. Photoelectron spectra for (**a**) 1.4×10^{14} Wcm^{-2}, (**b**) 3.1×10^{14} Wcm^{-2}, and (**c**) 5.7×10^{14} Wcm^{-2} in Ar. The numbers show the orders of the ATI peaks (separated by 5 eV). These data were obtained with an achromatic lens ($f = 300$ mm) at a pressure of 4.7×10^{-7} torr

2 Experimental results

Fig. 2 shows the photoelectron spectra in Ar, at peak intensities of (a) $1.4 \times 10^{14}\,\mathrm{Wcm}^{-2}$, (b) $3.1 \times 10^{14}\,\mathrm{Wcm}^{-2}$ and (c) $5.7 \times 10^{14}\,\mathrm{Wcm}^{-2}$. These data were obtained with an achromatic lens ($f = 300$ mm) at a pressure of 4.7×10^{-7} torr. The laser intensity was calibrated by measuring the short pulse resonant photoelectron spectrum of Ar as described later. The numbers show the order of the ATI peaks (separated by 5 eV). From the ion experiment, the saturation intensity is determined to be $\approx 5 \times 10^{14}\,\mathrm{Wcm}^{-2}$ [13]. The γ parameters of (a), (b), and (c) correspond to 3.1, 2.1, and 1.7 respectively. In this paper, we used the saturation intensity to estimate the γ parameter when the peak intensity exceeded the saturation intensity. The ionization occured in the multiphoton regime. Fig. 3 is replotted with the linear scale in the vertical axis of Fig. 2. The data in Fig. 3 were taken by changing the peak intensity by a factor of 4. In this range, the positions of the ATI peaks shift by 1.3 eV, at most, from what would be at the zero intensity ($Nh\nu - I_\mathrm{P} = 4.24$ eV). However, these positions do not shift with increasing intensity. This is consistent with the Stark-induced resonances picture of multiphoton ionization [10]. As the peak intensity increases beyond the appearance intensity, more resonances appear at the lower energy region, but the spectra maintain their general structure. Three photons will first come into resonance with the high-lying Rydberg levels, *ns* and *nd*, because of the ac Stark shift. Such resonances due to Rydberg series are the most prominent feature of short-pulse electron spectra [16]. Multiphoton ionization in the rare gases tends to favor ionization to the $^2P_{3/2}$ limit by more than what would be expected from a statistical argument [17, 18]. In Fig. 3a, the lower and higher energy peaks shift by 0.69 eV and 0.04 eV, respectively, from 4.24 eV. These offset energies are equal to the ac Stark shifts required for the resonances of the related levels. We can, therefore, assign the peaks to the 5*s* and 6*s* Rydberg levels, assuming that the high Rydberg levels have an ac Stark shift equal to the ponderomotive energy [19, 20]. Each of these peaks arise from the volume where the laser intensities match exactly to those required for resonance [10, 21]. The behavior of the 5*s* and 6*s* peaks is the same as quoted in [10] where the positions and the widths of the ATI peaks did not change. In Fig. 3b, a new peak appears on the low energy side. Because the ac Stark shift, required for the resonance, is 1.3 eV, we assigned the peak to the 3*d* state in good agreement with the measurement. In this case, the ac Stark shift is equal to the ponderomotive potential at the peak laser intensity. Therefore, we can calibrate the peak intensity from the appearance of the 3*d* peak. In Fig. 3c, the new distribution on the low energy side appeared. This energy spread could be due either to electrons from Ar^+ or to unresolved peaks of sublevels of the 3*d* and 3*d*′ states. Six sublevels are possibly in resonance with three photons, assuming the selection rule for the angular momentum *J* [7]. The spacings between the sublevels are smaller than the resolution (≈ 150 meV).

Fig. 4 shows the photoelectron spectra in Ne, at intensities of (a) $2.5 \times 10^{14}\,\mathrm{Wcm}^{-2}$, (b) $7.9 \times 10^{14}\,\mathrm{Wcm}^{-2}$ and (c) $4.0 \times 10^{15}\,\mathrm{Wcm}^{-2}$. The results in Figs. 4a and 4b were obtained with an achromatic lens ($f = 300$ mm), and in Fig. 4c with an off-axis parabolic mirror ($f = 125$ mm) at a pressure of 4.7×10^{-7} torr. From the ion experiment, the saturation intensity is determined to be $\approx 3 \times 10^{15}\,\mathrm{Wcm}^{-2}$ [13]. The γ parameters of (a), (b), and (c) correspond to 2.7, 1.5, and 0.79, respectively. The ionization occured in the multiphoton regime except for Fig. 4c. Figure 5 is replotted with the linear scale in the vertical axis of Fig. 4. The ATI peak (2.0 eV) in Figs. 5a and 5b shifts by 1.4 eV from the position of 3.43 eV at the zero intensity. We assigned this peak to the four-photon resonance with the $3p$ Rydberg levels, assuming that the p

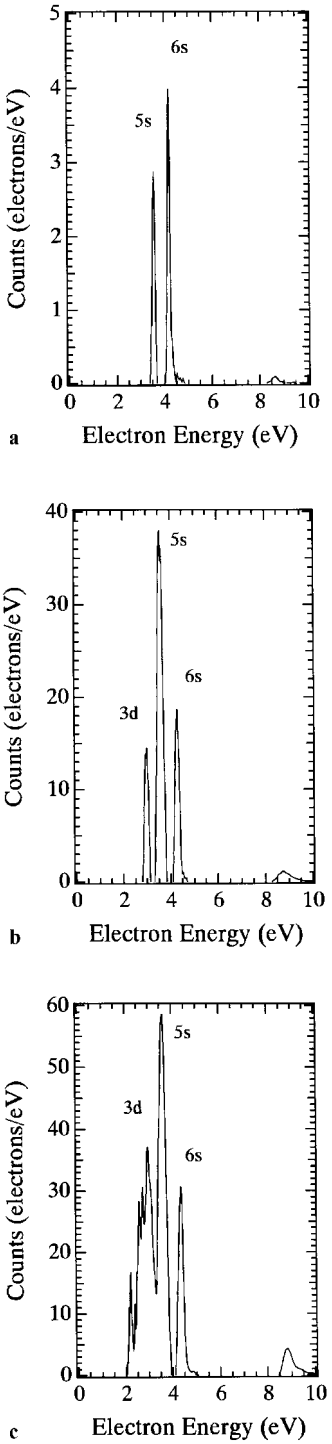

Fig. 3a–c. Replot with the linear scale from the vertical axis of Fig. 2 with an emphasis on the first peak. These conditions are the same as those in Fig. 2

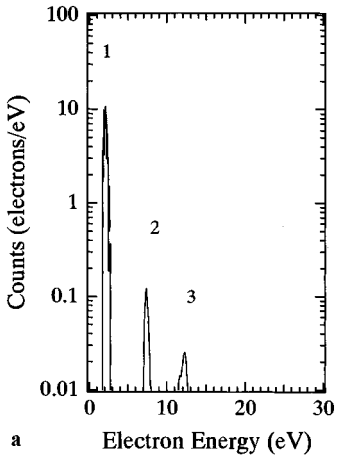

a

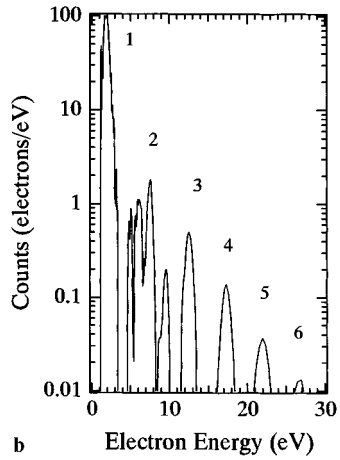

b

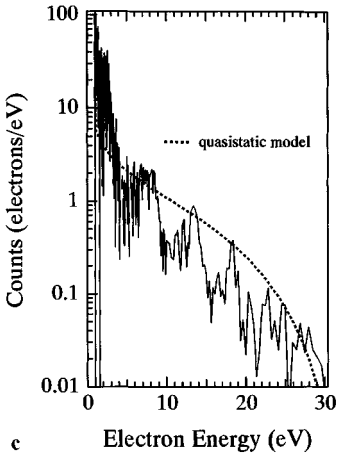

c

Fig. 4a–c. Photoelectron spectra for (**a**) 2.5×10^{14} Wcm^{-2}, (**b**) 7.9×10^{14} Wcm^{-2}, and (**c**) 4.0×10^{15} Wcm^{-2} in Ne. The data in (**a**) and (**b**) were obtained with an achromatic lens ($f = 300$ mm), and (**c**) was obtained with an off-axis parabolic mirror ($f = 125$ mm) at a pressure of 4.7×10^{-7} torr

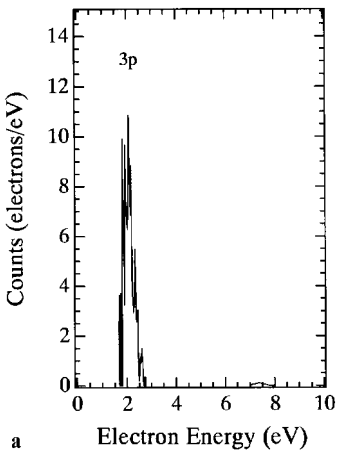

a

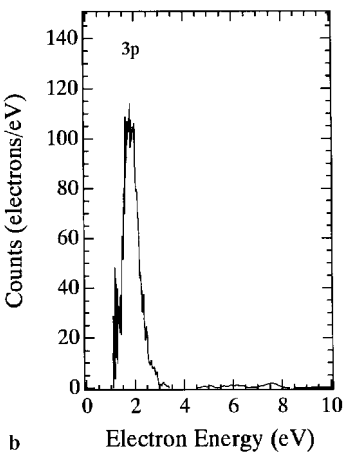

b

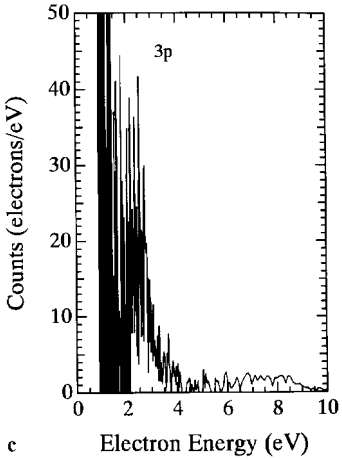

c

Fig. 5a–c. Replot using the linear scale from the vertical axis of Fig. 4 with an emphasis on the first peak. These conditions are the same as those in Fig. 4

Rydberg series has an ac Stark shift equal to the ponderomotive energy. The ac Stark shift, required for the resonance with the $3p$ state series (1.3–1.4 eV), is in good agreement with the observed value (1.4 eV).

The widths of the first peaks in (a) and (b) are 0.40 eV (FWHM) and 0.65 eV (FWHM), respectively. This fact contradicts the feature of resonance ionization described in [10] where the widths are quite small and do not depend on laser intensity. The broad widths could be due to the four photon-allowed sublevels of the $3p$ and $3p'$ states. The intensity broadening may arise from the onset of tunneling ionization. The exact reason was not made clear from this experiment.

In Fig. 4b, the new peaks appear between the first and second ATI peak. We assigned the 4.9 eV peak to the three-photon resonance with the $7d$ Rydberg levels. However, the origin of the 6 eV peak is unclear because it does not cor-

respond to the resonance, and the contribution from Ne^+ is ruled out in this intensity.

In Fig. 4c, the photoelectron energy spectrum shows the continuum, while the feature of the discrete peaks barely remains. The growth of the continuum is not due to ponderomotive acceleration, collisions, or space-charge effects because it was not observed in Ar at the same intensity. This spectrum is strongly reminiscent of those in the long wavelength limit, that is, of field or tunnel ionization. In the low frequency limit, ionization is explained by a quasi-instantaneous process leaving the free electron with zero velocity [1]. The final kinetic energy of electrons is determined by the classical motion in the electromagnetic field and the time at which the electron is created. For linearly polarized light, the residual kinetic energy of photoelectrons is distributed from zero to $2U_P$ continuously. In Fig. 4c, the calculation at an intensity of $3.1 \times 10^{15}\,\mathrm{Wcm^{-2}}$ ($U_P = 18$ eV) by the quasistatic model is fitted to the data. This figure shows the evolution from the multiphoton to tunneling regime as γ decreases, even in the UV wavelength region.

Fig. 6 shows the photoelectron spectra in He, at intensities of (a) $6.8 \times 10^{14}\,\mathrm{Wcm^{-2}}$, (b) $1.6 \times 10^{15}\,\mathrm{Wcm^{-2}}$, and (c) $6.5 \times 10^{15}\,\mathrm{Wcm^{-2}}$. The results in Figs. 6a and 6b were obtained with an achromatic lens ($f = 300$ mm), and in Fig. 6c with an off-axis parabolic mirror ($f = 125$ mm) at a pressure of $\approx 4 \times 10^{-7}$ torr. Hence, the saturation intensity of ionization is $4.7 \times 10^{15}\,\mathrm{Wcm^{-2}}$ [12]. In He, the γ parameter of (a), (b), and (c) correspond to 1.8, 1.2, and 0.73, respectively. In Fig. 6a and b, the ATI peaks are not prominent even though $\gamma > 1$. Some substructures still seem to be present in the spectra. This may be because of the broad resonances; that is, the five-photon resonance with the nf and np series and the four-photon resonance with the 2s state. The ac Stark shifts are 4.1–4.7 eV ($4f - 7f$), 1.4–4.7 eV ($2p - 7p$), and 0.23 eV ($2s$). If these resonances are allowed, the energy spread of the ATI peaks is enough to cover the energy separation (5 eV). Another reason is that the contribution of the tunneling ionization appears already. In Fig. 6c, the electron spectrum, which extends to 30 eV, does not show the ATI structure. The chaotic spikes are not reproducible. The spectrum clearly shows the feature of tunneling ionization at $\gamma < 1$. The calculation by the quasistatic model at an intensity of $3.5 \times 10^{15}\,\mathrm{Wcm^{-2}}$ ($U_P = 20$ eV) is shown in Fig. 6c.

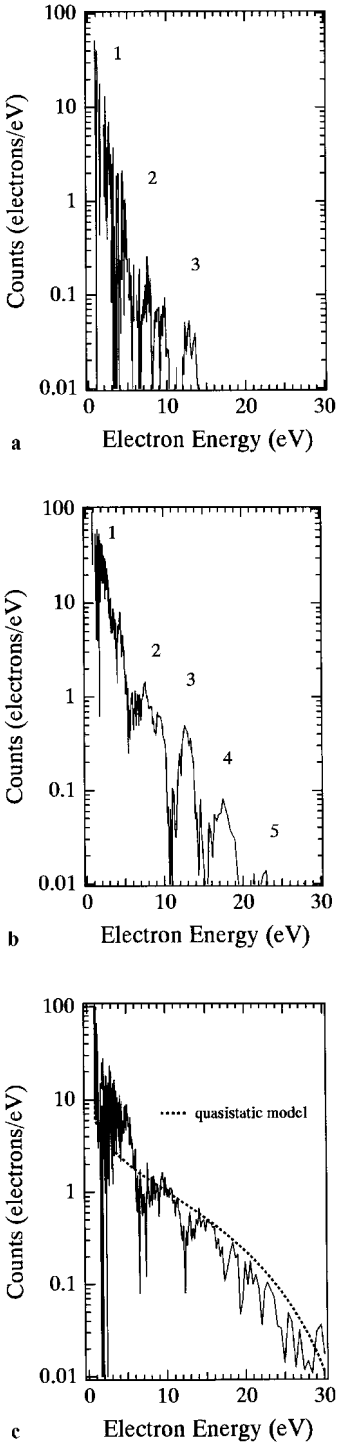

Fig. 6a–c. Photoelectron spectra for (**a**) $6.8 \times 10^{14}\,\mathrm{Wcm^{-2}}$, (**b**) $1.6 \times 10^{15}\,\mathrm{Wcm^{-2}}$, and (**c**) $6.5 \times 10^{15}\,\mathrm{Wcm^{-2}}$ in He. Data in (**a**) and (**b**) were obtained using an achromatic lens ($f = 300$ mm), and in (**c**) using an off-axis parabolic mirror ($f = 125$ mm) at a pressure of 4.7×10^{-7} torr

3 Discussion

Luk et al. [9] explained the broadening of ATI peaks by the ponderomotive shift combined with the dynamics of ion population. In their study, non-resonant ionization was assumed and the linewidth was determined by the difference in U_P between the appearance intensity of ionization and the peak laser intensity. Figure 3 shows a clear resonance structure. Each peak does not shift as the laser intensity increases. The results of this paper apparently contradict [9].

The positions and widths of the 5s and 6s peaks in Ar agree well with those observed by a short-pulse XeCl laser [10]. However, the width of the 3p peak in Ne is quite broad and depends on laser intensity. This result differs from [10]. This broadening is tentatively explained by the contribution of the sublevels of the 3p state and by the onset of tunneling ionization. The broad ATI peaks were observed in He even when $\gamma > 1$. This was attributed to the many possible resonances or the contribution of tunneling ionization. In Ne and He, the evolution from ATI peaks to the continuum was observed as γ decreases to less than 1.

4 Summary

We observed the photoelectron spectra in a strong KrF laser field. In Ar, the ATI peaks were observed clearly and their positions did not shift with laser intensity. This fact can be explained by the Stark-induced resonances and we assigned the peak to the 5*s*, 6*s* and 3*d* state. In Ne and He, these resonance structures were broadened with increasing laser intensity. Finally, these resonance peaks merged into the continuum. Tunneling ionization is dominant at $\gamma < 1$ in the UV wavelength as well as in the long wavelength.

References

1. N.H. Burnett, P.B.Corkum: J. Opt. Soc. Am. B **6**, 1195 (1989)
2. B.E. Lemoff,G.Y. Yin, G.L. Gordon III, C.P.J. Barty, S.E. Harris: Phys. Rev. Lett. **74**, 1574 (1995)
3. Y. Nagata, K. Midorikawa, S. Kubodera, M. Obara, H. Tashiro, K. Toyoda: Phys. Rev. Lett. **71**, 3774 (1993)
4. L.V. Keldysh: Zh. Eksp. Teor. Fiz. **47**, 1945 (1964), Sov. Phys. JETP **20**, 1307 (1965)
5. E. Mevel, P. Breger, R. Trainham, G. Petite, P. Agostini, A. Migus, J. P. Chambaret, A. Antonetti: Phys. Rev. Lett. **70**, 406 (1993)
6. S. Augst, D.D. Meyerhofer, D. Strickland, S.L. Chin: J. Opt. Soc. Am. B **8**, 858 (1991)
7. O.L. Landen, M. D. Perry, E. M. Campbell: Phys. Rev. Lett. **59**, 2558 (1987)
8. M.D. Perry, A. Szoke, K. C. Kulander: Phys. Rev. Lett. **63**, 1058 (1989)
9. T.S. Luk, T. Graber, H. Jara, K. Boyer, C.K. Rhodes: J. Opt. Soc. Am B **4**, 847 (1987)
10. G.N. Gibson, R.R. Freeman, T.J. Mc Ilrath: Phys. Rev. Lett. **69**, 1904 (1992)
11. Y. Nabekawa, K. Kondo, N. Sarukura, K Sajiki, S. Watanabe: Opt. Lett. **18**, 1922 (1993)
12. K Kondo, A. Sagisaka, T. Tamida, Y. Nabekawa, S. Watanabe: Phys. Rev. A **48**, R2531 (1993)
13. K. Kondo, T. Tamida, Y. Nabekawa, S. Watanabe: Phys. Rev. A **49**, 3881 (1994)
14. A. Sagisaka, Y. Nabekawa, K. Kondo, S. Watanabe: Appl. Phys. B **61**, 217 (1995)
15. S. Watanabe, K. Kondo, Y. Nabekawa, a Sagisaka, Y. Kobayashi: Phys. Rev. Lett. **73**, 2692 (1994)
16. R.R. Freeman, P.H. Bucksbaum: J. Phys. B **24**, 325 (1991)
17. P.H. Bucksbaum, L.D. van Woerkom, R.R. Freeman, D.W. Schumacher: Phys. Rev. A **41**, 4119 (1990)
18. T.J. Mc Ilrath, P.H. Bucksbaum, R.R. Freeman, M. Bashkansky: Phys. Rev. A **35**, 4611 (1987)
19. R.R. Freeman, P.H. Bucksbaum, H. Milchberg, S. Darack, D. Schumacher, M.E. Geusic: Phys. Rev. Lett. **59**, 1092 (1987)
20. P. Agostini, P. Breger, A. L'Huillier, H.G. Muller, G. Petite, A. Antonetti, A. Migus: Phys. Rev. Lett. **63**, 2208 (1989)
21. T.J. Mc Ilrath, R.R. Freeman, W.E. Cooke, L.D. van Woerkom: Phys. Rev. A **40**, 2770 (1989)